

Investigation on the Binding Effect of Cytochrome P450cam to Adrenodoxin by Using Computational Approach

A. Rozaq, T.P.M. Yunaz, M.A. Putri, S. Khairi, Z. Al-Fatony, R. Lubis, D. Jumbianti, A. Napitupulu, H. Sudrajat, C. Riani, T.R. Furlani and A. Bintarti

Ikatan Mahasiswa Eksakta Indonesia, Sekip Utara, Sleman,
Yogyakarta 55281, Daerah Istimewa Yogyakarta, Indonesia

Abstract: Binding effect of cytochrome P450cam to adrenodoxin has been investigated. Combined QM/MM calculations of an active site of Cytochrome P450cam have been performed, before and after a binding process of Cytochrome P450cam to Adrenodoxin. The calculations have been carried out for two coordination spheres of the heme active-site of Cytochrome P450cam, namely a 5-coordinated and a 6-coordinated system of this protein having a water molecule as a 6th ligand. An experimentally observed increase of a Fe-S stretching frequency after the binding process of Cytochrome P450cam to Adrenodoxin, has been reproduced in our calculations. The best agreement between the experiment increase and the theoretical increase of this vibrational frequency was found in our calculations for the 6-coordinated heme active-site.

Key words: QM/MM method • DFT • Cytochrome P450cam • Adrenodoxin

INTRODUCTION

Cytochrome P450cam catalyses the regio- and stereo-specific hydroxylation reaction of a substrate (deamphor) at physiological conditions [1]. The catalytic activity of P450cam has been intensively characterized by experimental [2-17] and theoretical [18-29] studies, therefore P450cam became a model protein for the entire class of P450 enzymes. The hydroxylation reaction of deamphorin P450cam requires a water molecule, molecular oxygen and two electrons to proceed [30]. Both electrons are transferred in two distinct steps into a reaction site of the enzyme, after the binding process of P450cam to Adrenodoxin (AdR) [31-36]. Both experimental [37,38] and theoretical [39,40] studies suggest that AdR binds to P450cam from the proximal side of the heme active-site of Cytochrome, forming a grid of hydrogen bonds between both proteins. In a recent experimental study, the resonance raman spectroscopy has been used to probe the binding effect of P450cam to AdR [37]. In the investigation a change of the frequency of the heme Fe-S stretching vibration has been observed, confirming that the binding process of P450cam to AdR, takes place from the proximal side of the P450cam enzyme. Although the perturbation of the P450cam active-site by the presence of AdR, was a subject of extensive investigations, a molecular mechanism of the interaction between both proteins remains still unknown.

A few computational studies have been devoted to the binding process of P450cam to AdR [39,40], presenting its global description. These studies showed an importance of hydrogen bonds between both proteins and an importance of an electrostatic interaction between them. However because of a limitation of the theory used in these calculations, they were unable to consider electronic effects, which seem to be the most important factors of the binding process. Therefore, to elucidate a mechanism of perturbation of the P450cam active-site after the binding process of this enzyme to AdR, we present here a computational study, which is based on a combined quantum mechanical-molecular mechanical (QM/MM) approach. In our calculations the heme active-site of P450cam and both its axial ligands, namely a distal water molecule and a proximal cysteine CYS357, were calculated at a QM level of theory, while the rest of the protein environment was calculated at a MM level. The results of our combined QM/MM calculations were compared with experimental resonance raman spectra of the P450cam active-site before and after the binding process of this enzyme to AdR. In the calculations, both coordination spheres of P450cam iron were considered, namely the 5-coordinated system and the 6-coordinated system having a water molecule as the 6th ligand. The calculations were performed for a doublet electronic state, according to experimental EPR evidence [2] suggesting

the low-spin character of the heme active-site in these protein systems particularly after the binding process of P450cam to AdR.

MATERIALS AND METHODS

MM Dynamics: We started from the x-ray experimental structure of cyanide (CN) complex of P450cam [17], as implemented in the 1O76 pdb protein file. We have chosen this experimental protein structure because it has a relatively high experimental resolution published so far (1.8 Å) and also it represents the same protein system which has been used in the resonance raman experiment (*escherichia coli* bacteria). Hydrogen atoms, which are missing in the x-ray structure, have been added to their standard positions according to the AMBER force field [41]. MM parameters for the heme active-site have been taken from the literature [42], however MM parameters of a camphor molecule, which is a part of the heme pocket of P450cam, have been obtained using the ANTECHAMBER program of the AMBER-8 programming suite. The protein system having the active site with 6-coordinated iron has been constructed in our calculations by replacing the CN ligand of the heme active-site by a water molecule. To neutralize the entire protein system, we have used 17 sodium counter-ions which positions have been obtained from electrostatic potential calculations using the AMBER program. Next, the protein system has been placed into a center of a water sphere, having explicit TIP3P water molecules [43]. The size of the water sphere was big enough to prevent all protein atoms to be at least 12 Å from the water-gas phase interface.

The MM dynamics consisted of slow 100 ps heating from 0 to 300 K performed at constant volume, followed by a long 10 ns equilibration dynamics performed at constant volume and constant temperature. In the simulation, we have applied a strong external harmonic potential of the value of 10 kcal/mol Å² outside the water sphere, keeping water molecules inside the sphere and a weak harmonic potential of the value of 1 kcal/mol Å², for sodium counter-ions. Separately, we have also performed the MM dynamics of the protein having the heme active-site with 5-coordinated iron, where the CN ligand has been completely removed. The MM dynamics for this protein system has been performed according to the same procedure, as the MM dynamics of the 6-coordinated protein system. Next we have performed the MM simulations of protein systems having P450cam bound to AdR. Despite many efforts, AdR has not been yet crystallized, therefore the x-ray structure of AdR has been taken from its protein mutation [44] as implemented in the 1OQQ pdb file. Serins 73 and 85 in this protein mutation have been replaced back in our calculations by cysteins,

to mimic the original wild type AdR. MM parameters of the 2Fe-2S component of the protein have been estimated from quantum mechanical calculations of this molecule bound to four-SH groups, mimicking binding of the 2Fe-2S molecule to the protein in the original protein structure of AdR. The quantum mechanical calculations of the 2Fe-2S-4SH complex has been performed at the B3LYP/6-31+G* level of theory in the gas phase. Hydrogen atoms which are missing in the original x-ray structures of AdR have been placed in standard positions using the AMBER program. Next AdR has been placed close to P450cam at the proximal side of the heme active-site of P450cam keeping the distance 12 Å from the iron atom of P450cam to one of iron atoms of AdR. The distance 12 Å which was used in our calculations, is consistent with previous MM simulations of the P450cam bound to AdR [39,40]. The protein complex of P450cam and AdR created in our study, has been placed into a center of a TIP3P water sphere, similar as in the MM simulations of P450cam alone. The size of the water sphere was large enough to keep all protein atoms inside the sphere at the distance at least 12 Å from the water-gas phase interface. Similar as in the MM simulations of P450cam alone, in the MM simulations of the protein complex we have applied a strong harmonic potential (10 kcal/mol Å²) outside the water sphere and a weak harmonic potential (1 kcal/mol Å²) for sodium counterions. The MM dynamics of the protein complex consisted of a slow 100 ps heating from 0 to 300 K, which was performed at constant volume keeping the distance between the iron atom of P450cam and one of the iron atoms of AdR, constrained to the value of 12 Å. After constrained heating, we have released the inter-protein constraint between the iron atoms of P450cam and AdR and we have performed the long MM equilibration dynamics for a period of 10 ns at constant volume and constant temperature.

Combined QM/MM Calculations: After the MM simulations, 10 protein snapshots have been randomly selected from each MM dynamics between 9.0ns to 10.0ns of a dynamics time. Each selected protein snapshot has been minimized at the MM level of theory using the AMBER program. Because of a big size of the protein system used in the MM dynamics, the MM energy minimizations have been performed with all water molecules constrained. Then each selected protein snapshot has been divided into a QM part and a MM part of the system. The QM part included the heme molecule and proximal cysteine CYS357 and the MM part included the rest of the protein system and the water sphere. For the systems which involve the 6-coordinated heme active-site, the QM part included also the water molecule. A chemical bond between CYS357 and the protein has been

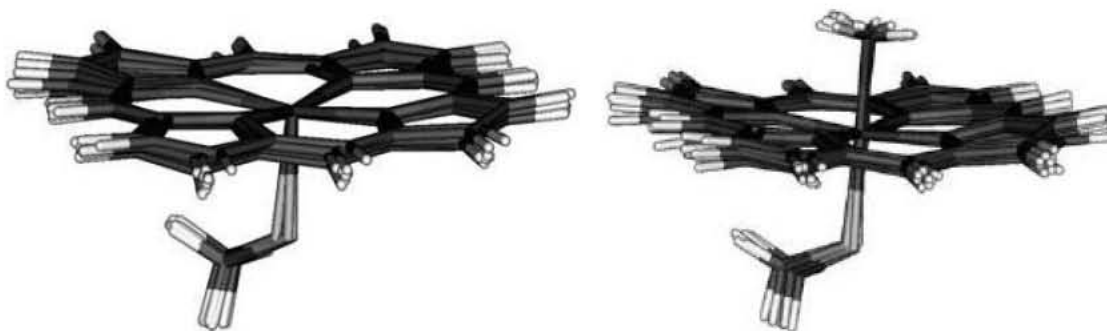


Fig. 1: Optimal geometries of the 5-coordinated and 6-coordinated heme active-site obtained in the QM/MM calculations for the doublet electronic state, based on 10 protein snapshots after MM dynamics of Cytochrome P450cam

Table 1: The properties of the Fe-S and Fe-O bonds obtained from the QM/MM calculations in Cytochrome P450cam and in the protein complex of Cytochrome P450cam and Putidaredoxin (Pdx), for the 5-coordinated and the 6-coordinated heme activesite in the doublet electronic state

Doublet electronic state	P450cam	P450cam/AdR	Change in protein
5-coord. heme			
Fe Charge (a.u.)	-0.47(± 0.05)	-0.52(± 0.12)	-0.05
S Charge (a.u.)	0.21(± 0.05)	0.36(± 0.03)	0.15
Fe-S distance (Å)	2.21(± 0.01)	2.16(± 0.03)	-0.05
Fe-S freq. (cm^{-1})	354(± 9)	385(± 10)	31
6-coord. heme			
Fe Charge (a.u.)	-0.75(± 0.20)	-0.49(± 0.23)	0.26
S Charge (a.u.)	0.16(± 0.05)	0.12(± 0.04)	-0.04
Fe-S distance (Å)	2.25(± 0.04)	2.22(± 0.05)	-0.03
Fe-O distance (Å)	2.01(± 0.02)	2.02(± 0.03)	0.01
Fe-S freq. (cm^{-1})	360(± 14)	376(± 11)	16
Fe-S exp. freq. (cm^{-1})*		350.5	353.5 3

The "Change in protein" column presents a difference between results of calculations performed in the protein complex of Cytochrome P450cam/AdR and in Cytochrome P450cam alone. The atomic charges are calculated according to the net Mulliken population. The results of the calculations are average values based on 10 protein snapshots obtained after MM dynamics. The rms errors of these average values are given in brackets. The calculated frequencies are scaled by a factor 0.92, which reflects a common characteristic of the DFT method [51]. *Experimental data are taken from reference [37].

cut and resulting free chemical valences have been filled out by hydrogen atoms according to the link atom method [45,46]. Then the QM system has been simplified by eliminating side chains of the heme molecule and side chains of CYS357, analogous as it has been done by others in similar calculations of heme proteins [47,48]. The QM models used in our calculations for the 5-coordinated and 6-coordinated active-sites are shown in Figures 1. Next the geometry of the QM part of the system has been optimized without any constraints inside the fixed MM part of the system. The geometry optimization of the QM system has been performed at the B3LYP/6-31+G* level of theory, while the MM protein environment was

represented by the AMBER force field. In the QM/MM calculations all external point charges (MM atoms of a protein and a water sphere) of the MM protein environment have been included in evaluation of the QM electronic wave function. The interaction between QM and MM atoms has been approximated by a classic Lennard-Jones potential, using newly developed parameters [49]. After geometry optimization, oscillation Hessian has been calculated of the same QM system in the same MM fixed protein matrix, using the same QM/MM procedure. The QM/MM calculations were carried out using the commercial software package Q-Chem [50] and the results are presented Table 1 as average arithmetic values based on 10 protein snapshots obtained from the MM dynamics. Rms errors of these average values are reported in brackets.

RESULTS AND DISCUSSION

Table 1 presents the results of the our combined QM/MM calculations for the doublet electronic state of the system with the 5-coordinated and 6-coordinated heme active-sites in the protein, based on the MM dynamics of P450cam and the protein complex of P450cam and AdR. According to our results for the 5-coordinated heme activesite, the Fe-S stretching frequency increases by 31 cm^{-1} after the binding process of P450cam to AdR. Although the calculated increase of the vibrational frequency is much bigger than the experimental increase of this frequency (3 cm^{-1}), our results show a correct trend in the frequency change of this vibration after the binding process of P450cam to AdR. Results of our QM/MM calculations present also that the increase of the Fe-S oscillation frequency is accompanied with a decrease of the Fe-S bond calculations is decreased by the value of 0.05 Å after the binding process of P450cam to AdR. There are also observed in our calculations changes of

electron density, mainly of the sulfur atom of the heme active-site of P450cam. According to Mulliken populations obtained in our QM/MM calculations, there is a decrease of electron density on the sulfur atom by the value of 0.15 a.u. However the decrease of electron density on the sulfur atom is not compensated by the increase of electron density on the iron atom, which indicates that after the binding process of P450cam to AdR, there is an electron density transfer from the sulfur atom to other atoms of the heme ring.

Similar as for the protein system having the 5-coordinated heme active-site, we observe in our calculations for the system with the 6-coordinated heme active-site, that the frequency of the Fe-S stretching vibration becomes bigger by a value of 16 cm⁻¹, after the binding process of P450cam to AdR. We observe also in our calculations that the change of the Fe-S frequency is accompanied with the change of the Fe-S inter-atomic distance, which becomes shorter by a value of 0.03 Å. In contrast, the Fe-O bond length becomes systematically bigger after the binding process of P450cam to AdR, however the elongation of the Fe-O bond has the value of only 0.01 Å. A different trend in the electron density distribution is observed in our calculations for the 6-coordinated active-site than it has been observed for the 5-coordinated active-site. According to Mulliken populations of heme iron for the 6-coordinated active-site, there is observed in our calculations a decrease of the electron density on iron by the value of 0.26 a.u. The electron density on the sulfur atom however remains relatively unchanged and we do not observe in our calculations a significant change of electron density on the water ligand of the heme active-site. Therefore we conclude that binding process of P450cam to AdR causes the electron density transfer from iron to other atoms of the heme ring, increasing the electron density of the heme ring, similar as it has been observed for the protein system with the 5-coordinated center.

We observe in our QM/MM calculations a general trend in the change of Fe-S bond properties after the binding process of P450cam to AdR, namely the frequency of the Fe-S stretching vibration becomes bigger and the Fe-S bond length becomes smaller. This effect is observed in our calculations for both the 5-coordinated and the 6-coordinated heme active-site. The correlation of both changes in the Fe-S bond properties, indicates that after the binding process of P450cam to AdR, the size of the proximal side of the heme pocket becomes smaller. In the smaller heme pocket, there are stronger steric interactions between atoms of the heme active-site and proximal atoms of the protein environment and as a

consequence, the Fe-S bond length becomes smaller and the frequency of the Fe-S stretching vibration becomes bigger. However, according to our calculations, the size of the distal side of the heme pocket remains unchanged or even becomes bigger. This conclusion is supported in our calculations by an observation that for the 6-coordinated system the Fe-O bond becomes longer. The binding process of P450cam to AdR changes also the electrostatic potential of the heme pocket of P450cam, however this effect is more complex. According to our calculations, there is an electron density transfer from the sulfur atom to other atoms of the heme ring, which appears for the 5-coordinated heme active-site and a similar electron density transfer is observed from the iron atom of the 6-coordinated heme active-site. However, we do not observe significant changes of the electron density on the water ligand of the 6-coordinated heme active site. Therefore we assume that after the binding process of P450cam to AdR, there is a systematic increase of the electron density of other atoms in the heme ring. It is also interesting to compare the results of our calculations of the 5-coordinated active-site with the results of the calculations of the 6-coordinated system, in order to distinguish which coordination center is dominant in the proteins. According to results of our study, we have found very similar results of the absolute values of the Fe-S oscillation frequencies obtained in our calculations for both coordination sites of heme iron. However, the increase of the Fe-S vibrational frequency obtained in the calculations for the 6-coordinated system (16 cm⁻¹) is closer to experimental data (3 cm⁻¹) than the frequency increase of the 5-coordinated heme active-site (31 cm⁻¹). Therefore, we conclude that the 6-coordinated iron center, having the water molecule as the axial ligand, seems to be dominant in P450cam before and after the binding process of this enzyme to AdR.

We observe also in our calculations an interesting change in the properties of the Fe-O bond of the 6-coordinated heme active site. The binding process of P450cam to AdR changes the electrostatic field of the heme pocket which decreases the electron density on heme iron. The decrease of electron density on iron is accompanied in our calculations with the elongation of the bond between iron and the water ligand and as a consequence, it can increase activity of binding and releasing of any distal ligand to iron in P450cam. This observation can explain the experimentally observed activity of the P450cam enzyme, after the binding process of this enzyme to AdR. However, this effect requires additional computational studies of P450 proteins and therefore it is a subject of our current investigation.

CONCLUSIONS

Combined QM/MM calculations of the P450cam active-site in the doublet electronic state are presented, before and after the binding process of P450cam to AdR. The calculations are based on MM dynamics of P450cam and a protein complex of P450cam with AdR. In the calculations we have considered two coordination spheres of heme iron, namely the 5-coordinated and the 6-coordinated heme active-site having a water molecule as the 6th ligand. We have reproduced in our calculations an experimentally observed increase of the Fe-S oscillation frequency after the binding process of P450cam to AdR. According to results of our calculations, there is a better agreement with experiment for the 6-coordinated heme active-site than for the 5-coordinated system. Therefore we conclude that the 6-coordinated heme active-site seems to be dominant in the investigated protein systems. We have also observed in our study, that the increase of the Fe-S oscillation frequency is accompanied with the decrease of the Fe-S bond length, after the binding process of P450cam to AdR. This change of the Fe-S bond properties has been found in our study for both coordination spheres of heme iron. We conclude that the change of the Fe-S bond properties, is related the geometry change of a proximal side of the heme pocket, which becomes smaller after the binding process of both proteins. In contrast, we also observe in our calculations a systematic elongation of the Fe-O bond for the 6-coordinated heme active-site of P450cam. The calculated change of the Fe-O bond length indicates that the size of the distal side of the heme pocket remains unchanged or even becomes slightly bigger. We have also found in our calculations that the binding process of both proteins causes an electron density transfer from heme sulfur to other atoms of the heme ring for the 5-coordinated system and the similar electron density transfer from heme iron to other atoms of the heme ring for the 6-coordinated active-site. However, for the 6-coordinated heme active-site, we do not observe a significant change of the electron density on the water ligand after the binding process. Finally, we conclude that the change of electron density distribution along atoms of the heme active-site, is related to a change of an electrostatic potential of the heme pocket. For the 6-coordinated heme active-site, the electron density on heme iron becomes smaller and the bond between iron and the water ligand becomes longer. This observation can explain a bigger catalytic activity of P450cam in processes involving ligand bonding or ligand releasing, after the binding process of this enzyme to AdR. However this issue requires additional computational investigations of the P450 family and it is a subject of our current studies.

REFERENCES

1. Mueller, E.J., P.J. Loida and S.G. Sligar, 1995. "Cytochrome p450 Structure, Mechanism and Biochemistry", R.P. Ortiz de Montellano Ed. Plenum Press, New York,
2. Lipscomb, J.D., *Biochem.*, 1980. Vol. 19, pp:3590-3599.
3. Poulos, T.L., B.C. Finzel, I.C. Gunsalus, G.C. Wagner and J. Kraut, 1985. *J. Biol. Chem.*, 30: 16122-16130.
4. Raag, R. and T.L. Poulos, 1989. *Biochem.*, 28: 7586-7592.
5. Shiro, Y., T. Iizuka, R. Makino, Y. Ishimura and I. Morishima, 1989. *J. Am. Chem. Soc.*, 111: 7707-7711.
6. Simianu, M.C. and J.R. Kincaid, 1995. *J. Am. Chem. Soc.*, 117: 4628-4636.
7. Li, H., S. Narasimhulu, L.M. Havran, J.D. Winkler and T.L. Poulos, 1995. *J. Am. Chem. Soc.*, 117: 6297-6299.
8. Mouro, C., A. Bondon, G. Simonneaux and C. Jung, 1997. *FEBS Lett.*, 414: 203-208.
9. Vidakovic, M., S.G. Sligar, H. Li and T. Poulos, 1998. *Biochem.*, 37: 9211-9219.
10. Davydov, R., I.D.G. Macdonald, T.M. Makris, S.G. Sligar and B.M. Hoffman, 1999. *J. Am. Chem. Soc.*, 121: 10654-10655.
11. Mouro, C., A. Bondon, C. Jung, J.D. De Certaines and G. Simonneaux, 2000. *Eur. J. Biochem.*, 267: 216-221.
12. Schichting, I., J. Berendzen, K. Chu, A.M. Stock, S.A. Maves, D.E. Benson, R.M. Sweet, D. Ringe, G.A. Petsko and S.G. Sligar, 2000. *Sci.*, 287: 1615-1622.
13. Davydov, R., T.M. Makris, V. Kofman, D.E. Werst, S.G. Sligar and B.M. Hoffman, 2001. *J. Am. Chem. Soc.*, 123: 1403-1415.
14. Deng, T., I.D.G. Macdonald, M.C. Simianu, M. Sykora, J.R. Kincaid and S.G. Sligar, 2001. *J. Am. Chem. Soc.*, 123: 269-278.
15. Yoshioka, S., T. Tosha, S. Takahashi, K. Ishimori, H. Hori and I. Morishima, 2002. *J. Am. Chem. Soc.*, 124: 14571-14579.
16. Jin, S., T.M. Makris, T.A. Bryson, S.G. Sligar and J.H. Dawson, 2003. *J. Am. Chem. Soc.*, 125: 3406-3407.
17. Fedorov, R., D.K. Ghosh and I. Schlichting, 2003. *Arch. Biochem. Biophys.*, 409: 25-31.
18. Zakhariyeva, O., A.X. Trautwein and C. Veeger, 2000. *Biophys. Chem.*, 88: 11-34.
19. Ogliaro, F., S. Cohen, S.P. de Visser and S. Shaik, 2000. *J. Am. Chem. Soc.*, 122: 12892-12893.
20. Yoshizawa, K., Y. Kagawa and Y. Shiota, 2000. *J. Phys. Chem. B.*, 104: 12365-12370.
21. Goller A.H. and T. Clark, 2001. *J. Mol. Struct. (Theochem)*, 541: 263-281.
22. Yoshizawa, K., T. Kamachi and Y. Shiota, 2001. *J. Am. Chem. Soc.*, 123: 9806-9816.

23. Schoneboom, J.C., H. Lin, N. Reuter, W. Thiel, S. Cohen, F. Ogliaro and S. Shaik, 2002. *J. Am. Chem. Soc.*, 124: 8142-8151.
24. Kamachi T. and K. Yoshizawa, 2003. *J. Am. Chem. Soc.*, 125: 4652-4661.
25. Bathelt, C.M., L. Ridder, A.J. Mulholland and J.N. Harvey, 2003. *J. Am. Chem. Soc.*, 125: 15004-15005.
26. de Visser, S.P., D. Kumar, S. Cohen, R. Shacham and S. Shaik, 2004. *J. Am. Chem. Soc.*, 126: 8362-8363.
27. Kumar, D., S.P. de Visser and S. Shaik, 2004. *J. Am. Chem. Soc.*, 126: 5072-5073.
28. Meunier, B., S.P. de Visser and S. Shaik, 2004. *Chem. Rev.*, 104: 3947-3980.
29. Schoneboom, J.C., S. Cohen, H. Lin, S. Shaik and W. Thiel, 2004. *J. Am. Chem. Soc.*, 126: 4017-035.
30. Brewer, C.B. and J.A. Peterson, 1988. *J. Biol. Chem.*, 263: 791-798.
31. Lipscomb, J.D. S.G. Sligar, M.J. Namtvedt and I.C. Gunsalus, 1976. *J. Biol. Chem.*, 251: 1116-1124.
32. Sjodin, T., J.F. Christian, I.D.G. Macdonald, R. Davydov, M. Unno, S.G. Sligar, B.M. Hoffman and P.M. Champion, 2001. 40: 6852-6859.
33. Tosha, T., S. Yoshioka, S. Takahashi, K. Ishimori, H. Shimada and I. Morishima, 2003. *J. Biol. Chem.*, 278: 39809-39821.
34. Pochapsky, S.S., T.C. Pochapsky and J.W. Wei, 2003. *Biochem.*, 42: 5649-5656.
35. Nagano, S., T. Tosha, K. Ishimori, I. Morishima and T.L. Poulos, 2004. *J. Biol. Chem.*, 279: 42844-42849.
36. Tosha, T., S. Yoshioka, K. Ishimori and I. Morishima, 2004. *J. Biol. Chem.*, 279: 42836-42843.
37. Unno, M., J.F. Christian, D.E. Benson, N.C. Gerber, S.G. Sligar and P.M. Champion, 1997. *J. Am. Chem. Soc.*, 119: 6614-6620.
38. Unno, M., J.F. Christian, T. Sjodin, D.E. Benson, I.D.G. Macdonald, S.G. Sligar and P.M. Champion, 2002. *J. Biol. Chem.*, 277: 2547-2553.
39. Pochapsky, T.C., T.A. Lyons, S. Kazanis, T. Arkaki and G. Ratnaswamy, 1996. *Biochimie*, 78: 723-733.
40. Roitberg, A.E., M.J. Holden, M.P. Mayhew, I.V. Kurnikov, D.N. Beratan and V.L. Vilker, 1998. *J. Am. Chem. Soc.*, 120: 8927-8932.
41. Case, D.A. D.A. Pearlman, J.W. Caldwell, T.E. Cheatham III, W.S. Ross, C.L. Simmerling, T.A. Darden, K.M. Merz, R.V. Stanton, A.L. Cheng, J.J. Vincent, M. Crowley, V. Tsui, R.J. Radmer, Y. Duan, J. Pitera, M. Massova, G.L. Seibel, U.C. Singh, P.K. Weiner and P.A. Kollman, 2004. *AMBER 8*, University of California, San Francisco.
42. Giammona, D.A., 1984. Ph.D. thesis, University of California, Davis.
43. Jorgensen, W.L., J. Chandrasekhar, J.D. Madura, R.W. Impley and M.L. Klein, 1983. *J. Chem. Phys.*, 79: 926-935.
44. Sevrioukova, I.F., C. Garcia, H. Li, B. Bhaskar and T.L. Poulos, 2003. *J. Mol. Biol.*, 333: 377-392.
45. Singh, U.C. and P.A. Kollman, 1986. *J. Comput. Chem.*, 7: 718-730.
46. Field, M.J., P.A. Bash and M. Karplus, 1990. *J. Comput. Chem.*, 11: 700-733.
47. Spiro, T.G., M.Z. Zgierski and P.M. Kozlowski, 2001. *Coord. Chem. Rev.*, 219: 923-936.
48. Sigfridsson, E. and U. Ryde, 2002. *J. Inorg. Biochem.*, 91: 101-115.
49. Freindorf, M., Y. Shao, T.R. Furlani and J. Kong, 2005. *J. Comput. Chem.*, 26: 1270-1278.
50. Kong, J., C.A. White, A.I. Krylov, D. Sherrill, R.D. Adamson, T.R. Furlani, M.S. Lee, A.M. Lee, S.R. Gwaltney, T.R. Adams, C. Ochsenfeld, A.T.B. Gilbert, G.S. Kedziora, V.A. Rassolov, D.R. Maurice, N. Nair, Y. Shao, N.A. Besley, P.A. Maslen, J.P. Dombrowski, H. Daschel, W. Zhang, P.P. Korambath, J. Baker, E.F. C. Byrd, T.V. Voorhis, M. Oumi, S. Hirata, C.P. Hsu, N. Ishikawa, J. Florian, A. Warshel, B.G. Johnson, P.M. W. Gill, M. Head-Gordon and J.A. Pople, 2000. *J. Comput. Chem.*, 21: 1532-1548.
51. Rauhut, G. and P. Pulay, 1995. *J. Phys. Chem.*, 99: 3093-3100.